



ACCEPTED MANUSCRIPT

This is an early electronic version of an as-received manuscript that has been accepted for publication in the Journal of the Serbian Chemical Society but has not yet been subjected to the editing process and publishing procedure applied by the JSCS Editorial Office.

Please cite this article as A. V. Gasimzade, V. Kh. Nurullayev, and R. R. Khalilzade, *J. Serb. Chem. Soc.* (2026) <https://doi.org/10.2298/JSC260309032G>

This “raw” version of the manuscript is being provided to the authors and readers for their technical service. It must be stressed that the manuscript still has to be subjected to copyediting, typesetting, English grammar and syntax corrections, professional editing and authors’ review of the galley proof before it is published in its final form. Please note that during these publishing processes, many errors may emerge which could affect the final content of the manuscript and all legal disclaimers applied according to the policies of the Journal.



J. Serb. Chem. Soc. **00(0)** 1-23 (2026)
JSCS-13830

Chemical technology aspects of non-equilibrium microwave heating for phase separation in multiphase liquid systems

AYSEL V. GASIMZADE^{1*}, VALI KH. NURULLAYEV², AND RASHAD R. KHALILZADE¹

¹Azerbaijan State Oil and Industry University, Baku, Azerbaijan, and ²State Oil Company of Azerbaijan Republic, Baku, Azerbaijan.

(Received 9 March; revised 7 May; accepted 11 June 2026)

Abstract: Microwave-assisted demulsification is a promising method for separating water-in-oil emulsions because it provides rapid and volumetric energy transfer. However, the mechanism of separation under non-equilibrium heating conditions remains insufficiently understood. In this study, the kinetic factors governing microwave-assisted phase separation were investigated at microwave powers of 200–800 W and water fractions of 0.12–0.45. Temperature evolution, heating rate (dT/dt), separated water volume, and specific energy consumption were analysed. The results showed a pronounced non-monotonic dependence of separation efficiency on microwave power. The highest separation efficiency was observed at intermediate powers of 400–600 W, while further power increases reduced performance despite continued temperature rise. The findings demonstrate that heating rate, rather than final temperature, is the main controlling parameter, providing a basis for more energy-efficient microwave demulsification.

Keywords: dielectric heating; heating-rate control; specific energy consumption; contour optimization; kinetic destabilization.

INTRODUCTION

Water–oil emulsions are an unavoidable consequence of crude oil production, particularly in mature reservoirs where the water cut increases and fluids remain in contact for extended periods. Under such conditions, natural surface-active components of crude oil promote the formation of dispersed systems that are kinetically stable and difficult to separate. These emulsions complicate transportation, reduce processing efficiency, and increase energy consumption in surface facilities. Their behavior is controlled not only by temperature, but also by interfacial properties, phase distribution, and the time-dependent response of the system.^{1–3} In industrial practice, separation is commonly achieved through thermal

* Corresponding author. E-mail: gasimzade92@inbox.ru
<https://doi.org/10.2298/JSC260309032G>

treatment and chemical demulsifiers.⁴⁻⁶ While these methods are widely used, they often require elevated temperatures or substantial chemical dosages, which increase operational costs and raise environmental concerns. For this reason, there is growing interest in physical methods that can enhance separation efficiency without excessive energy input or chemical dependency.⁷⁻¹¹

Microwave heating provides a distinct alternative to conventional conductive heating. Instead of transferring heat from the surface inward, microwave energy is deposited directly within the volume of the material and interacts preferentially with polar components.¹²⁻¹⁵ In heterogeneous systems such as water-in-oil emulsions, where the dispersed and continuous phases possess different dielectric properties, this selective interaction can lead to localized heating and transient non-uniform conditions. As a result, the structural response of the emulsion cannot be described solely by its average temperature.¹⁶⁻¹⁹ The efficiency of microwave-assisted separation depends on several coupled parameters, including applied power, heating rate, phase connectivity, and interfacial relaxation dynamics. When energy input is balanced with structural relaxation, phase separation is enhanced, whereas excessive power or rapid heating may increase molecular mobility and reduce coalescence efficiency.²⁰⁻²¹ Although this study uses crude oils from the Absheron oilfields, the analysis is based on general physical parameters, making the approach applicable to a wide range of water-in-oil systems in petroleum processing.²²⁻²⁶

In this study, water-in-oil emulsions prepared from Absheron crude oils were subjected to controlled microwave irradiation at power levels between 200 and 800 *W*. Systems with different water volume fractions were examined. Temperature evolution, heating rate, separated water volume, and specific energy consumption were evaluated in order to identify operating conditions that promote efficient phase separation. By linking separation performance to both kinetic behaviour and energy input, the work aims to clarify the mechanisms governing microwave interaction with multiphase liquid systems. From a mechanical and industrial engineering standpoint, microwave-assisted demulsification can be regarded as an energy-driven separation process in which power delivery and dynamic response play a more decisive role than bulk temperature alone.

EXPERIMENTAL

The experimental methodology was designed to evaluate the influence of microwave power and emulsion structure on phase separation under controlled laboratory conditions. Water-in-oil emulsions prepared from Absheron crude oils with different water fractions were subjected to controlled microwave irradiation, and their heating behavior, separation efficiency, and energy consumption were analyzed.²⁷⁻³³

Materials and sample preparation. Crude oil samples were obtained from producing wells No. 533, 623, 629, and 628 located in the Absheron oilfields (Azerbaijan), representing mature onshore reservoirs with moderate density and elevated resin-asphaltene content that promote stable water-in-oil emulsions. The oils were stored in sealed glass containers at 20 °C and

protected from light prior to use, while distilled water ($\text{pH} \approx 5.5$) was used as the dispersed phase. Emulsions were prepared at controlled water volume fractions ($\phi = 0.12\text{--}0.45$) by mixing oil and water with a mechanical impeller at 2000 rpm for 8–10 min at 20 °C, followed by a short stabilization period. The emulsion type was verified using the standard drop-dispersion test, confirming that all systems were water-in-oil (W/O). The internal structure of the emulsions varied with water fraction, evolving from isolated droplets at low ϕ to partially connected networks at intermediate fractions and highly connected structures at high water content. For microwave experiments, 70 ± 0.5 g of emulsion was transferred into a 100 mL borosilicate glass beaker used as the standard sample container.^{27–30}

Microwave treatment procedure. Microwave irradiation was performed using a laboratory-scale microwave reactor (Milestone ETHOS microwave reactor, Italy) operating at a fixed frequency of 2.45 GHz. The output power was adjustable and set to four discrete levels: 200, 400, 600, and 800 W. Experiments were conducted in an open reaction vessel under atmospheric pressure conditions. The emulsion sample (70 ± 0.5 g) placed in a 100 mL borosilicate glass beaker was positioned at the geometric center of the microwave cavity using a non-metallic holder to ensure reproducible electromagnetic exposure. Each sample was irradiated for a predetermined time interval controlled with an accuracy of ± 0.5 s. Temperature–time profiles were monitored during microwave irradiation. The temperature of the emulsion was monitored using a calibrated K-type thermocouple (accuracy ± 0.1 °C). Immediately after irradiation (within 2–3 s), the bulk temperature of the emulsion was measured. The probe was inserted along the central axis of the sample to a depth of approximately 15 mm below the surface to minimize surface-related temperature deviations. All experiments were carried out under identical geometric and environmental conditions to ensure reliable comparison of heating behavior and phase separation efficiency across different microwave power levels.^{31–33}

Dielectric characterization methodology. To further evaluate the electromagnetic response of the emulsions during microwave-assisted heating, additional dielectric characterization was performed for W/O systems with different water fractions ($\phi = 0.12\text{--}0.45$). The dielectric constant (ϵ'), dielectric loss factor (ϵ''), dissipation factor ($\tan\delta$), and effective microwave wavelength (λ_{eff}) were determined under microwave treatment conditions corresponding to the main demulsification experiments. The analysis was carried out at microwave powers of 200, 400, 600, and 800 W using the bulk temperatures measured after 60 s of irradiation (T_{60}). The dielectric behavior of the aqueous phase, oil phase, and emulsion mixture was evaluated using temperature-dependent dielectric correlations commonly applied for heterogeneous liquid systems under microwave exposure. The obtained dielectric parameters were used to assess the influence of microwave power and water fraction on microwave energy absorption and dissipation behavior in the emulsion system^{34–36}.

Viscosity measurement methodology. To investigate the contribution of thermal-viscosity effects to microwave-assisted phase separation, viscosity measurements were additionally performed before and after microwave treatment. W/O emulsions with different water fractions ($\phi = 0.12\text{--}0.45$) were subjected to microwave irradiation at powers of 200–800 W under the same experimental conditions used in the demulsification tests. Following microwave exposure, the apparent dynamic viscosity of the emulsions was measured after thermal stabilization under controlled laboratory conditions. Viscosity reduction (%) was calculated relative to the initial viscosity of the untreated emulsion samples. The separated water volume obtained after microwave treatment was additionally recorded in order to evaluate the relationship between viscosity reduction and demulsification efficiency^{37–39}.

Interfacial tension methodology. To evaluate the influence of microwave irradiation on interfacial destabilization, the interfacial tension (IFT) of the W/O emulsions was measured before and after microwave treatment. Emulsions with different water fractions ($\phi = 0.12\text{--}0.45$) were treated at microwave powers of 200, 400, 600, and 800 W using the same irradiation conditions applied in the phase-separation experiments. Interfacial tension measurements were carried out under controlled temperature conditions using standard tensiometric procedures. The obtained IFT values were used to assess the effect of microwave power on interfacial properties and their possible relationship with phase separation behavior⁴⁰⁻⁴².

Energy consumption analysis. To evaluate the energetic performance of the microwave-assisted separation process, the specific energy consumption per unit volume of separated water (E/A / kWh/m³) was calculated.

The parameter E/A represents the electrical energy supplied to the system required to separate a unit volume of water from the emulsion and is commonly used for comparative assessment of thermal and electromagnetic separation processes⁴³. The specific energy consumption was determined using:

$$E/A = (P \cdot t) / A \quad (1)$$

where P is the microwave power / kW, t is the irradiation time / h, A is the separated water volume / m³.

Nominal microwave power levels (200–800 W) were converted to kilowatts for calculations. The irradiation time was measured experimentally for each test. The separated water volume was determined gravimetrically and converted to volumetric units under standard conditions. All energy calculations were performed under identical operating conditions to ensure consistency and reliable comparison between different power regimes.

RESULTS AND DISCUSSION

Microwave interaction with heterogeneous liquid systems arises from a coupled interplay between electromagnetic energy absorption, interfacial polarization phenomena, and phase-dependent thermal responses. In dispersed media composed of immiscible liquid phases, such as emulsions, microwave energy input induces spatially non-uniform heating and localized structural rearrangements that cannot be adequately captured by bulk temperature evolution alone. For this reason, elucidating the interdependence between applied microwave power, the resulting temperature increase, and phase separation behavior is critical for identifying the physical mechanisms that govern structural destabilization and phase evolution.

A substantial body of microwave demulsification studies illustrates enhanced phase separation with increasing supplied energy, achieved either through elevated power levels or prolonged irradiation durations, a behavior commonly attributed to viscosity reduction and accelerated droplet coalescence.

In the present study, by contrast, the structural response exhibits a pronounced non-monotonic character. Maximum separation is attained within an intermediate power range, beyond which further increases in power lead to a decline in separation efficiency despite continued temperature rise. Such behavior demonstrates that demulsification cannot be interpreted as a purely thermal

process; rather, it reflects a dynamic balance between microwave energy deposition and the rate of interfacial structural relaxation, as illustrated in Fig. 1.

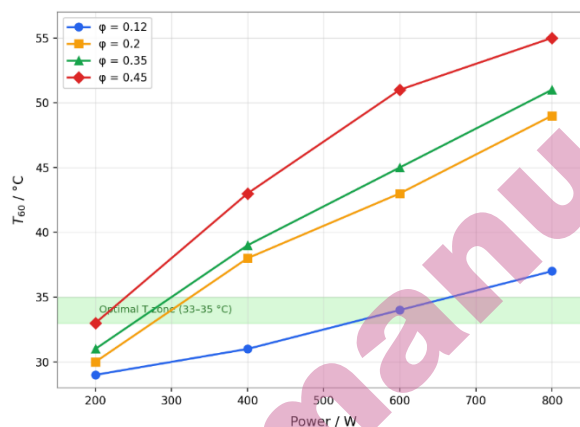


Fig. 1. Temperature at 60 s (T_{60}) versus microwave power for emulsions with $\phi = 0.12$ – 0.45 . Shaded region indicates the optimal temperature range.

Fig. 1 shows the dependence of bulk temperature measured after 60 s of microwave exposure on the applied power level for emulsions with varying water volume fractions. For all investigated systems, the bulk temperature increased progressively with increasing microwave power. However, the magnitude of the temperature rise appears to depend strongly on the water fraction of the emulsion.

At the lowest water content ($\phi = 0.12$), the temperature increase remained relatively moderate across the investigated power range. Even at 800 W, the bulk temperature reached only approximately 37 °C, which may be associated with limited microwave absorption due to the relatively low volume of the polar aqueous phase. Under intermediate power conditions, the emulsion remained within or near the experimentally observed temperature interval associated with favourable phase separation behaviour.

As the water fraction increased ($\phi = 0.20$ and 0.35), the temperature response became more pronounced. The larger dispersed aqueous phase likely enhanced dielectric losses and volumetric microwave energy absorption, resulting in higher apparent heating rates. At microwave powers of 600–800 W, the measured bulk temperature exceeded 45 °C, indicating intensified energy dissipation within the emulsion system.

For the highest water fraction ($\phi = 0.45$), the most significant temperature increase was observed, reaching approximately 55 °C at 800 W. This behaviour may be related to enhanced electromagnetic interaction associated with increased water-phase connectivity and interfacial density. At the same time, the results suggest that operation at excessively high microwave powers may shift the system

beyond the experimentally favourable temperature region for stable phase separation.

The shaded region in Fig. 1 highlights the temperature interval (33–35 °C) associated with relatively favourable demulsification behaviour under the investigated conditions. At moderate microwave powers (200–400 W), several emulsions passed through this interval, which may indicate a balance between interfacial destabilization and controlled molecular mobility. In contrast, at higher power levels the systems rapidly exceeded this temperature range, where excessive heating may contribute to increased phase mobility and less efficient droplet coalescence.

From a heat-transfer perspective, the results indicate that microwave heating behavior in heterogeneous emulsions depends strongly on dielectric composition and water fraction. Nevertheless, since the present analysis is based on bulk temperature measurements obtained after microwave irradiation, possible local thermal gradients and transient hot-spot formation could not be directly resolved. Therefore, the proposed interpretation of non-equilibrium heating effects should be considered as an indirect phenomenological interpretation derived from macroscopic experimental observations rather than direct local thermal characterization.

Although temperature remains a key parameter influencing phase stability—through its effects on interfacial tension, molecular mobility, and phase connectivity—its role under microwave irradiation cannot be considered in isolation. Rather, thermal effects are inherently coupled with kinetic and electromagnetic contributions, giving rise to strongly nonlinear responses. Identifying temperature ranges associated with effective structural transformation is therefore essential for elucidating the mechanisms governing microwave-induced phase separation, as further illustrated in Fig. 2.

Fig. 2 shows the relationship between separated water volume and bulk temperature after 60 s of microwave exposure for emulsions with different water fractions. The obtained results indicate that phase separation efficiency does not increase monotonically with temperature but instead exhibits a composition-dependent optimum behaviour.

At low water content ($\phi = 0.12$), phase separation remained relatively limited throughout the investigated temperature range, which may be associated with weaker dielectric interaction and lower microwave energy absorption due to the reduced amount of dispersed aqueous phase. For intermediate water fractions ($\phi = 0.20$ – 0.35), the separated water volume increased progressively within a moderate temperature interval, with the highest separation efficiency for $\phi = 0.35$ observed near approximately 45 °C before declining at higher temperatures.

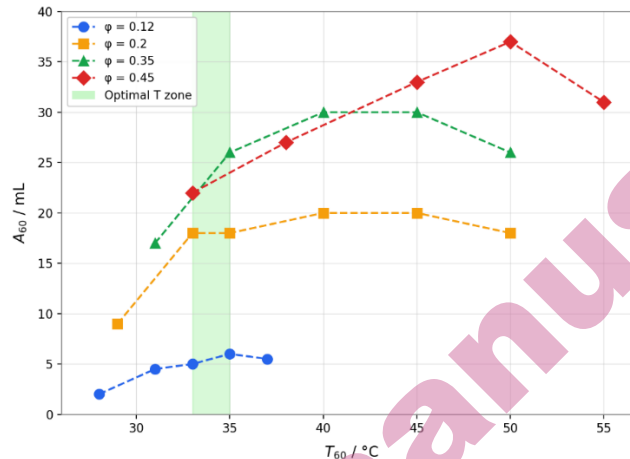


Fig. 2. Separated water volume (A) versus bulk temperature (T_{60}) for emulsions with $\phi = 0.12$ – 0.45 . Shaded region indicates the optimal range.

At the highest investigated water fraction ($\phi = 0.45$), phase separation initially increased rapidly with temperature but subsequently decreased beyond a certain temperature range. This behaviour may indicate that excessively rapid heating and increased phase mobility partially suppress stable droplet coalescence under high-energy microwave conditions.

The obtained results suggest that microwave-assisted demulsification may operate within a limited temperature and heating regime rather than following a purely temperature-controlled separation trend. At the same time, since the analysis was based primarily on bulk temperature measurements obtained after microwave irradiation, the possible influence of local thermal gradients, transient overheating, and non-uniform energy distribution could not be directly resolved. Therefore, the proposed interpretation should be considered as an indirect phenomenological explanation of the experimentally observed separation behaviour.

To further clarify the role of dynamic heating effects, the separation performance was analysed as a function of heating rate rather than bulk temperature alone. The heating rate (dT/dt) was determined from the temperature rise during the initial 60 s of microwave exposure. The relationship between separated water volume and heating rate for different water fractions is illustrated in Fig. 3.

Fig. 3 illustrates the relationship between separated water volume and apparent heating rate (dT/dt) for emulsions with different water fractions. The obtained results suggest that phase separation efficiency may be more strongly influenced by heating dynamics than by bulk temperature alone. For all investigated systems, an initial increase in heating rate was generally associated

with improved phase separation behaviour. However, beyond a certain range, further increases in heating rate did not result in proportional enhancement of separated water volume and, in several cases, led to reduced separation efficiency.

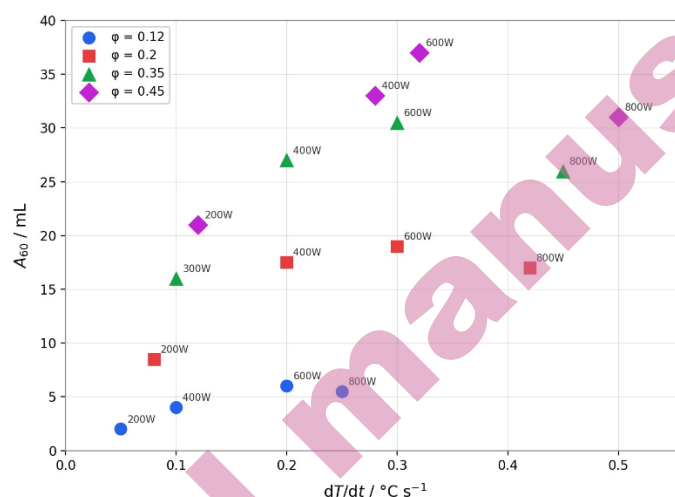


Fig. 3. Separated water after 60 s (A_{60}) versus heating rate (dT/dt) for emulsions with $\phi = 0.12$ – 0.45 . Power levels: 200–800 W.

At low water content ($\phi = 0.12$), the apparent heating rate remained relatively small across the investigated microwave power range, and only moderate improvement in separation efficiency was observed. This behaviour may be associated with limited dielectric losses and reduced interfacial area, which likely restrict the conversion of absorbed microwave energy into efficient droplet coalescence.

For intermediate water fractions ($\phi = 0.20$ and 0.35), a more pronounced optimum heating-rate region was observed. The separated water volume increased progressively as dT/dt increased from low to moderate values, reaching maximum separation efficiency at intermediate microwave powers (400–600 W). At the highest investigated heating rates corresponding to 800 W, a reduction in separated water volume became apparent despite continued energy input. This behaviour may indicate that moderate microwave heating promotes interfacial destabilization and droplet interaction, whereas excessively rapid heating could increase molecular mobility and partially suppress stable phase disengagement.

The emulsion with the highest water fraction ($\phi = 0.45$) exhibited the strongest apparent sensitivity to heating rate. Maximum separation efficiency was observed near approximately 0.4 – 0.45 $^{\circ}\text{C/s}$ (600 W), followed by a decline at higher heating rates. Although this behaviour may suggest the existence of an optimal dynamic heating regime for microwave-assisted demulsification, the present results should

be interpreted cautiously because the heating-rate analysis was derived from bulk temperature measurements rather than direct local thermal characterization.

From an engineering perspective, the obtained data indicate that the rate of microwave energy delivery may play an important role in determining phase separation behaviour. The results further suggest that separation efficiency depends not only on the total energy supplied to the system but also on the dynamic conditions under which energy is deposited into the heterogeneous emulsion structure. At the same time, possible local overheating effects, transient thermal gradients, and interfacial relaxation processes were not directly measured in the present study. Therefore, the proposed interpretation of non-equilibrium heating effects should be considered as an indirect phenomenological interpretation derived from macroscopic experimental observations.

Microwave-assisted demulsification has frequently been interpreted as a predominantly thermally driven process. Numerous studies report that increasing microwave power or irradiation time enhances separation efficiency due to selective heating of the aqueous phase, reduction in viscosity, and accelerated droplet coalescence. For example, Binner *et al.* (2014) demonstrated that selective dielectric heating of dispersed saline droplets generates localized thermal gradients that promote phase disengagement. In such interpretations, separation efficiency typically increases monotonically with supplied energy⁴⁴.

However, the present results contradict this simplified thermal paradigm. A distinct non-monotonic separation behaviour was observed: separation efficiency reached a maximum within an intermediate power window (approximately 400–600 W), while further power increase (800 W) resulted in reduced performance despite continued temperature rise. This behaviour indicates that microwave demulsification cannot be explained solely by bulk heating effects⁴⁵.

Studies such as Fang *et al.* (1989) suggest that microwave irradiation may alter interfacial electrostatic properties by modifying droplet surface charge and zeta potential. While these findings highlight the importance of interfacial destabilization mechanisms, they do not explicitly account for kinetic limitations associated with rapid energy deposition.³⁷

The present work extends beyond both purely thermal explanations (e.g., Binner) and electrostatic interpretations (e.g., Fang) by identifying heating rate (dT/dt) as a governing engineering parameter. The observed divergence between peak and final heating rates further demonstrates that microwave-assisted demulsification operates within a finite kinetic window controlled by the balance between electromagnetic energy input and structural relaxation time⁴⁵⁻⁴⁹.

Moreover, unlike earlier studies that primarily evaluate separation yield, this investigation introduces a multi-criteria optimization framework incorporating separation efficiency, productivity, and specific energy consumption. The resulting contour-based efficiency mapping demonstrates that maximum power

application does not correspond to maximum process efficiency. Instead, optimal performance occurs within a localized composition–power interaction region⁴⁷⁻⁴⁹.

These findings suggest that microwave demulsification should be interpreted as a non-equilibrium energy-controlled separation mechanism rather than a purely temperature-dominated process, offering a more rigorous engineering basis for industrial scale-up.

In order to distinguish the influence of microwave power intensity on separation dynamics, the temperature–separation relationship was examined separately for 400 W and 600 W operating conditions. These two regimes represent intermediate and elevated energy input levels, respectively, and allow evaluation of structural response under different heating intensities. The corresponding results are presented in Fig. 4.

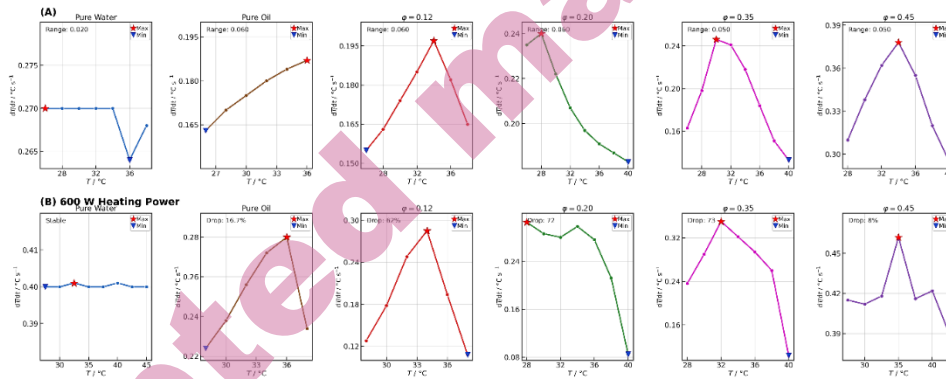


Fig. 4. Separated water volume (A_{60}) as a function of temperature at 400 W (A) and 600 W (B) for emulsions with different water fractions ($\phi = 0.12$ – 0.45).

Fig. 4 compares phase separation behaviour at two microwave power levels, 400 W and 600 W, illustrating the influence of microwave energy intensity on the temperature–separation relationship. At 400 W, separation efficiency exhibited a moderate and composition-dependent response, with relatively pronounced maxima observed for intermediate water fractions ($\phi = 0.20$ – 0.35) within a limited temperature interval.

At 600 W, the faster apparent heating conditions generally produced larger separated water volumes; however, the temperature interval associated with favourable separation behaviour became noticeably narrower, particularly for emulsions with $\phi = 0.35$ and 0.45 . In several cases, phase separation increased up to an intermediate temperature range and subsequently decreased despite continued temperature rise.

These observations suggest that increasing microwave power does not simply enhance demulsification efficiency in a linear manner but may additionally modify

the dynamic balance between microwave energy deposition, interfacial destabilization, and transient structural response of the emulsion system. Under higher-power conditions, excessively rapid heating may contribute to increased molecular mobility and less stable phase disengagement despite higher bulk temperatures.

At the same time, the present interpretation should be considered cautiously because the analysis was based primarily on bulk temperature measurements obtained after microwave irradiation. Direct characterization of local thermal gradients, transient hot spots, and structural relaxation phenomena was not performed. Therefore, the proposed interpretation represents an indirect phenomenological explanation of the experimentally observed separation behavior rather than direct mechanistic confirmation.

To further evaluate the dynamic characteristics of microwave heating under high power conditions, the peak heating rate and the final heating rate were compared as a function of water fraction at 600 W. This comparison allows assessment of transient versus stabilized heating behaviour and provides insight into structural relaxation effects during microwave exposure. The results are illustrated in Fig. 5.

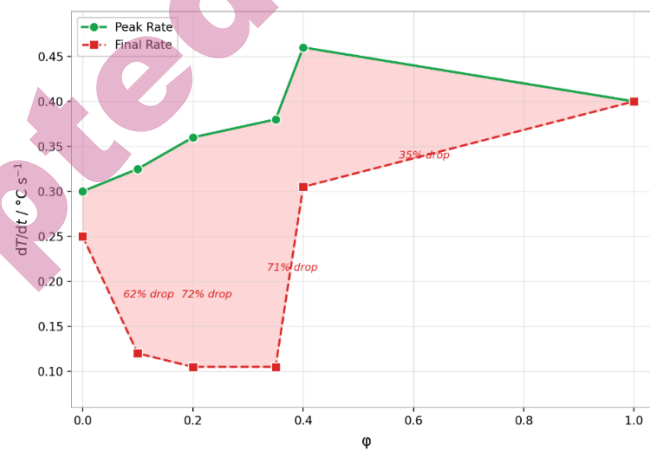


Fig. 5. Peak and final heating rates as a function of water fraction (ϕ) at 600 W.

Fig. 5 illustrates the variation of apparent peak and final heating rates with water fraction at a constant microwave power of 600 W. The obtained results show that the peak heating rate generally increased with increasing water fraction up to approximately $\phi \approx 0.45$, which may be associated with enhanced dielectric losses and stronger microwave energy absorption within the aqueous phase of the emulsion.

In contrast, the final heating rate exhibited a less uniform behavior, with a noticeable decrease relative to the peak heating rate at intermediate water fractions ($\phi \approx 0.12\text{--}0.35$). This behavior may indicate the presence of transient heating effects during microwave irradiation, where the initial energy absorption rate exceeds the subsequently stabilized thermal response of the system.

At higher water fractions ($\phi \geq 0.45$), the difference between peak and final heating rates became smaller, suggesting a comparatively more stable apparent energy absorption behavior under the investigated conditions. These observations indicate that transient heating dynamics may play an important role in microwave-assisted phase separation processes.

At the same time, the present interpretation should be considered cautiously because the heating-rate analysis was derived from bulk temperature measurements obtained after microwave irradiation rather than from direct local thermal monitoring. Consequently, possible local overheating effects, transient thermal gradients, and interfacial relaxation phenomena could not be directly resolved. Therefore, the proposed interpretation of transient structural response represents an indirect phenomenological explanation of the experimentally observed behavior rather than direct mechanistic verification.

To quantify the relative impact of microwave power on separation performance and energy efficiency, the percentage change in separated water volume and specific energy consumption (E/A) was evaluated with respect to the baseline condition (200 W). This comparative analysis enables assessment of performance gains and associated energy penalties across different water fractions. The results are summarized in Fig. 6.

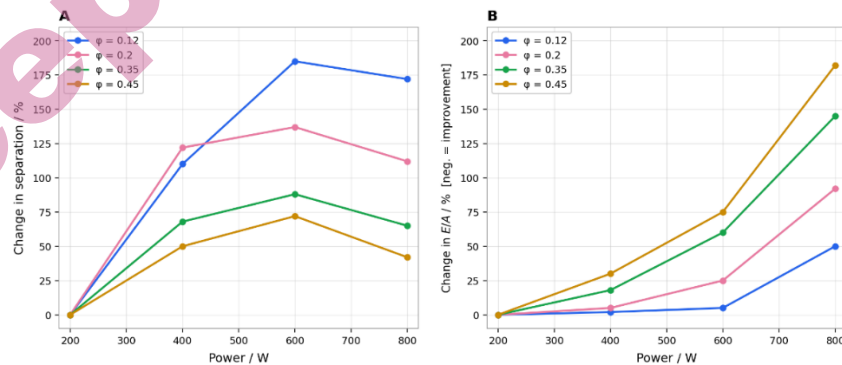


Fig. 6. Relative variation of (A) separated water (A) and (B) specific energy consumption (E/A) with microwave power for $\phi = 0.12\text{--}0.45$ (reference: 200 W).

Fig. 6 compares the influence of microwave power on phase separation efficiency and specific energy consumption for emulsions with different water fractions. The obtained results show that increasing microwave power from 200 to

400–600 W generally improved phase separation efficiency for all investigated systems. The strongest relative improvement was observed at low water content ($\phi = 0.12$), where the separated water volume increased substantially at intermediate microwave powers.

For intermediate water fractions ($\phi = 0.20$ – 0.35), separation efficiency also increased with microwave power; however, the improvement became less pronounced beyond approximately 600 W. At the highest investigated water fraction ($\phi = 0.45$), the increase in separation efficiency remained comparatively moderate despite continued power increase.

In contrast, the specific energy consumption increased significantly with increasing microwave power, particularly for emulsions with higher water fractions ($\phi = 0.35$ – 0.45). These results indicate that additional microwave energy input does not necessarily translate proportionally into improved phase separation performance under all operating conditions.

At the highest investigated microwave power (800 W), the increase in energy consumption became substantially more pronounced, whereas the corresponding separation improvement remained limited. This behaviour suggests that excessively high microwave power may reduce the overall energetic efficiency of the demulsification process despite continued temperature increase and intensified energy deposition.

From an engineering perspective, the obtained results suggest that favourable microwave-assisted demulsification performance may occur within an intermediate microwave power range of approximately 400–600 W under the investigated conditions. At the same time, since the present analysis was based on macroscopic measurements of bulk temperature, separated water volume, and energy consumption, possible local overheating effects and transient non-uniform energy redistribution could not be directly characterized. Therefore, the proposed interpretation should be considered as an indirect phenomenological assessment of the experimentally observed process behaviour rather than direct mechanistic verification.

To further clarify the role of electromagnetic interactions during microwave-assisted demulsification, additional dielectric characterization of the W/O emulsions was performed. Since microwave heating in heterogeneous systems is governed by selective interaction between the electromagnetic field and polar components, evaluation of dielectric parameters is essential for understanding the relationship between microwave power, energy absorption, and phase separation behaviour. For this reason, dielectric constant (ϵ'), dielectric loss factor (ϵ''), dissipation factor ($\tan\delta$), and effective microwave wavelength (λ_{eff}) were analysed for emulsions with different water fractions under microwave irradiation conditions. The measurements were carried out for microwave powers of 200–800

W using the temperature conditions corresponding to the experimental separation tests. The obtained dielectric parameters are summarized in Table I.

TABLE I. Dielectric parameters of W/O emulsions at different water fractions and microwave powers; φ – water volume fraction in the emulsion; T_{60} – bulk temperature measured after 60 s of microwave irradiation; ϵ' – dielectric constant; ϵ'' – dielectric loss factor; $\tan\delta$ – dielectric dissipation factor; λ_{eff} – effective microwave wavelength in the emulsion medium; W – microwave power unit; cm – wavelength unit.

Water fraction, φ	Power (W)	T_{60} (°C)	ϵ' water	ϵ'' water	ϵ' oil	ϵ'' oil	ϵ' mixture	ϵ'' mixture	$\tan\delta$ mixture	λ_{eff} (cm)
0.12	200	29.8	75.2	9.70	2.218	0.0068	3.42	0.025	0.0073	6.61
	400	33.6	73.9	8.60	2.216	0.0082	3.48	0.029	0.0083	6.55
	600	35.4	73.3	8.15	2.214	0.0090	3.51	0.032	0.0091	6.52
	800	37.0	72.8	7.80	2.213	0.0094	3.54	0.034	0.0096	6.49
0.20	200	31.6	74.6	9.15	2.217	0.0075	4.12	0.033	0.0080	6.04
	400	37.8	72.5	7.60	2.212	0.0088	4.25	0.040	0.0094	5.95
	600	43.5	70.6	6.60	2.208	0.0103	4.36	0.047	0.0108	5.87
	800	48.9	68.8	5.85	2.205	0.0106	4.45	0.052	0.0117	5.81
0.35	200	34.2	73.7	8.45	2.215	0.0085	5.24	0.041	0.0078	5.33
	400	42.8	70.8	6.69	2.209	0.0099	5.25	0.050	0.0095	5.32
	600	47.3	69.3	6.04	2.206	0.0104	5.22	0.051	0.0098	5.34
	800	54.0	67.1	5.27	2.201	0.0114	5.17	0.053	0.0103	5.36
0.45	200	36.2	73.0	7.95	2.214	0.0093	6.05	0.052	0.0086	4.96
	400	44.1	70.4	6.49	2.208	0.0106	6.12	0.060	0.0098	4.93
	600	50.4	68.3	5.66	2.203	0.0104	6.18	0.066	0.0107	4.91
	800	61.3	64.6	4.62	2.195	0.0130	6.26	0.074	0.0118	4.88

The dielectric analysis demonstrates that the electromagnetic response of the emulsion strongly depends on both water fraction and microwave power. The dielectric constant of the aqueous phase remained substantially higher than that of the oil phase throughout the investigated temperature range, confirming that microwave energy absorption occurs predominantly within the dispersed water domains. Simultaneously, the gradual increase in dielectric loss factor (ϵ'') and dissipation factor ($\tan\delta$) with increasing microwave power indicates intensified microwave energy conversion into heat within the heterogeneous emulsion structure.

The results further show that the dielectric properties of the emulsion evolve dynamically during heating. Although increased microwave power enhanced dielectric losses and energy dissipation, the highest phase separation efficiency was not observed at the maximum power level (800 W). This behaviour suggests that enhanced electromagnetic energy deposition alone cannot fully explain the observed demulsification behaviour. Instead, excessive power input may promote transient overheating and increased molecular mobility, which can partially suppress stable droplet coalescence.

At the same time, the present dielectric characterization represents averaged bulk behaviour of the emulsion system. Spatially resolved dielectric mapping and local electromagnetic field distribution were not directly measured. Therefore, the proposed interpretation of non-equilibrium microwave effects should be considered phenomenological rather than a direct mechanistic confirmation.

To evaluate whether the observed demulsification behavior can be explained solely by thermal-viscosity effects, additional viscosity measurements were performed before and after microwave treatment. Since viscosity strongly influences droplet mobility, collision frequency, and coalescence probability in W/O emulsions, investigation of viscosity evolution under microwave irradiation provides important insight into the contribution of thermal effects to phase separation. The experiments were carried out for emulsions with different water fractions at microwave powers of 200–800 W under the same irradiation conditions used in the separation experiments. The obtained viscosity values and corresponding separated water volumes are presented in Table II.

TABLE II. Influence of microwave power on viscosity reduction and phase separation efficiency of W/O emulsions; ϕ – water volume fraction in the emulsion; MW – microwave treatment; mPa·s – dynamic viscosity unit; W – microwave power unit; separated water – volume of water separated after microwave treatment.

Water fraction, ϕ	Microwave power (W)	Viscosity before MW (mPa·s)	Viscosity after MW (mPa·s)	Viscosity reduction (%)	Separated water (mL)
0.12	200	42.5	37.8	11.1	8.4
	400		32.4	23.8	13.9
	600		28.7	32.5	16.2
	800		24.1	43.3	15.4
0.20	200	58.7	49.5	15.7	15.8
	400		39.8	32.2	24.6
	600		33.2	43.4	29.1
	800		27.6	53.0	27.5
0.35	200	84.3	67.4	20.0	24.8
	400		50.1	40.6	33.9
	600		41.5	50.8	34.8
	800		32.6	61.3	31.2
0.45	200	116.8	89.5	23.4	30.5
	400		65.7	43.8	41.2
	600		52.4	55.1	46.7
	800		39.3	66.4	42.5

Microwave treatment resulted in a substantial reduction in emulsion viscosity for all investigated water fractions and power levels. The viscosity decrease became progressively more pronounced with increasing microwave power, reflecting enhanced thermal activation and reduced resistance to flow.

However, despite the continuous reduction in viscosity, the separated water volume did not increase monotonically at the highest microwave power level (800 W). In several systems, phase separation efficiency decreased even though viscosity reduction remained significant. This observation indicates that viscosity reduction alone cannot fully explain the demulsification behaviour under microwave irradiation.

The obtained results therefore support the assumption that microwave-assisted phase separation is influenced not only by thermal-viscosity effects but also by dynamic non-equilibrium phenomena associated with rapid energy deposition and transient interfacial restructuring. Excessively rapid heating may exceed the characteristic relaxation time of the emulsion structure, thereby limiting stable droplet coalescence despite lower viscosity values.

In order to further investigate the role of interfacial phenomena during microwave-assisted demulsification, the interfacial tension (IFT) of W/O emulsions was additionally analysed before and after microwave treatment. Since destabilization of the water–oil interface is one of the key factors controlling droplet coalescence and phase disengagement, evaluation of IFT variation under microwave exposure provides additional information regarding the contribution of interfacial effects to the separation process. The measurements were performed for emulsions with different water fractions treated at microwave powers of 200–800 W. The obtained results are illustrated in Fig. 7.

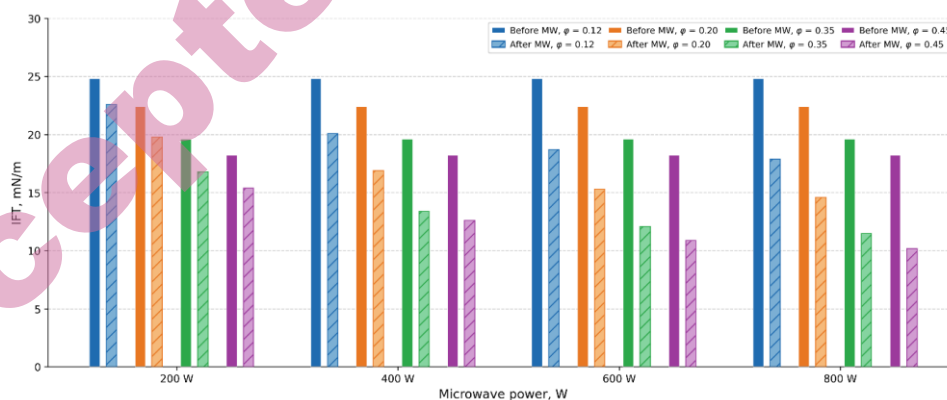


Fig. 7. Interfacial tension (IFT) of W/O emulsions with different water fractions before and after microwave treatment at different power levels.

The interfacial tension measurements additionally confirm that microwave irradiation promotes destabilization of the water–oil interface. For all investigated systems, interfacial tension decreased after microwave treatment, and the magnitude of reduction increased with microwave power.

Nevertheless, the decrease in interfacial tension did not correspond directly to maximum phase separation efficiency at the highest power level. Although the lowest IFT values were observed at 800 W, the separated water volume did not increase proportionally and, in some cases, decreased relative to intermediate power conditions.

This divergence suggests that interfacial tension reduction alone is insufficient to describe the complex behaviour of microwave-assisted demulsification. The results support the interpretation that the process is governed by a coupled interaction between dielectric energy absorption, heating dynamics, and transient structural response of the emulsion system.

To integrate the effects of power input and composition into a unified performance framework, an efficiency optimization map was constructed. The map combines separation yield and specific energy consumption into a single energy-efficiency metric and illustrates its dependence on microwave power and oil concentration. The resulting performance landscape is shown in Fig. 8.

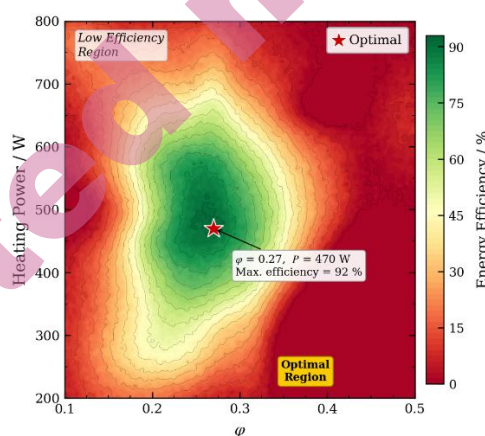


Fig. 8. Energy efficiency contour map as a function of water fraction (ϕ) and microwave power. The marked point indicates the optimal condition.

Fig. 8 presents the energy-efficiency contour map as a function of water volume fraction (ϕ) and microwave power. The obtained contour distribution indicates that process efficiency does not increase monotonically with either parameter. Instead, a localized efficiency maximum appears within an intermediate region of water fraction and microwave power.

The highest apparent efficiency was observed near $\phi \approx 0.27$ and $P \approx 470$ W, where η_{\max} reached approximately 92% under the investigated experimental conditions. This region may correspond to a comparatively favourable balance between microwave energy absorption, dielectric response, and phase-separation dynamics within the emulsion system.

At lower microwave powers (<300 W), the supplied energy appeared insufficient to achieve efficient destabilization of the water–oil interface, resulting in relatively limited phase separation across the investigated compositions. In contrast, at higher microwave powers (>700 W), the overall efficiency decreased despite continued energy input and elevated bulk temperatures. This behaviour may indicate that excessively rapid heating contributes to increased molecular mobility and less efficient phase disengagement while simultaneously increasing specific energy consumption.

The influence of water fraction also exhibited a non-linear behavior. At low water fractions, the reduced dielectric contrast likely limited effective microwave coupling and energy absorption. At high water fractions, increased phase connectivity and structural complexity may have reduced efficient phase disengagement under high-energy conditions. Consequently, the experimentally favourable operating region appeared within intermediate emulsion compositions, where microwave absorption and phase destabilization remained relatively balanced.

The contour map was constructed using interpolated experimental data within the investigated parameter range. Therefore, the identified optimal condition should be interpreted as an approximate practical operating region rather than a strict theoretical maximum. In addition, because the present analysis was based primarily on bulk thermal and separation measurements, local thermal gradients, transient electromagnetic field redistribution, and microscopic interfacial processes were not directly characterized.

From a process-engineering perspective, the obtained results suggest that microwave-assisted demulsification may be more effectively operated within a controlled efficiency window rather than at maximum available microwave power. Proper selection of both microwave power and emulsion composition appears important for achieving a favourable balance between phase separation performance and energy consumption under the investigated conditions.

Although the present study demonstrates clear relationships between microwave power, dielectric behaviour, viscosity reduction, interfacial tension variation, and phase separation efficiency, several limitations should be acknowledged. The kinetic analysis was primarily based on bulk temperature measurements obtained immediately after microwave irradiation. Direct spatial characterization of local temperature gradients, transient hot spots, droplet evolution, and interfacial charge redistribution was not performed.

Consequently, the proposed mechanisms related to structural relaxation, transient overheating, and non-equilibrium destabilization should be interpreted as indirect phenomenological interpretations derived from macroscopic experimental observations. Further investigations involving infrared thermal imaging, dielectric

field mapping, and in situ droplet-size characterization are required for direct mechanistic validation.

CONCLUSION

1. The obtained results indicate that microwave-assisted demulsification does not appear to follow a purely temperature-driven mechanism under the investigated conditions. The combined analysis of bulk temperature evolution, dielectric behaviour, viscosity reduction, interfacial tension variation, and phase separation efficiency suggests that heating dynamics may play an important role in determining demulsification performance. The experimentally favourable phase separation behaviour was observed mainly at intermediate microwave powers of approximately 400–600 W. At higher microwave power levels (≈ 800 W), separation efficiency decreased despite continued increases in bulk temperature, dielectric losses, viscosity reduction, and interfacial tension reduction. This behaviour may indicate that excessively rapid microwave heating contributes to transient non-equilibrium effects and less efficient phase disengagement.
2. The combined evaluation of separation yield, productivity, dielectric response, and specific energy consumption showed that the most favourable operating region under the investigated conditions occurred at intermediate water fractions ($\phi \approx 0.20$ – 0.35) and moderate-to-high microwave powers (≈ 470 – 600 W). The obtained contour-based efficiency analysis suggests that maximum microwave power input does not necessarily correspond to maximum process efficiency. Instead, efficient microwave-assisted demulsification appears to require a balanced interaction between microwave energy absorption, heating dynamics, and emulsion structure.
3. At the same time, the present analysis was based primarily on macroscopic measurements, including bulk temperature evolution, dielectric characteristics, viscosity, interfacial tension, and separated water volume. Direct characterization of local thermal gradients, transient hot spots, droplet evolution, and interfacial relaxation phenomena was not performed. Therefore, the proposed interpretation of non-equilibrium microwave effects should be considered as an indirect phenomenological interpretation derived from experimental observations rather than direct mechanistic confirmation. Further studies involving spatial thermal mapping, in situ droplet-size analysis, and localized dielectric characterization are required for more detailed mechanistic validation of microwave-assisted phase separation processes.

Acknowledgements: This work was carried out within the framework of the research program on corrosion mitigation in microbiologically active oilfield environments conducted at Azerbaijan State Oil and Industry University in collaboration with the State Oil Company of

Azerbaijan Republic (SOCAR). The authors gratefully acknowledge the technical support provided during electrochemical and microbiological testing. The authors also thank colleagues for valuable discussions related to impedance analysis and adsorption modelling.

ИЗВОД

ТЕХНОЛОШКИ АСПЕКТИ НЕРАВНОТЕЖНОГ МИКРОТАЛАСНОГ ЗАГРЕВАЊА У ЦИЉУ ФАЗНОГ РАЗДВАЈАЊА ВИШЕФАЗНИХ ТЕЧНИХ СИСТЕМА

AYSEL V. GASIMZADE¹, VALI KH. NURULLAYEV² AND RASHAD R. KHALILZADE¹¹Azerbaijan State Oil and Industry University, Baku, Azerbaijan, and ²State Oil Company of Azerbaijan Republic, Baku, Azerbaijan.

Микроталасно потпомогнута деемулгација представља перспективну методу за раздвајање емулзија типа вода-у-уљу, јер омогућава брз пренос енергије по целој запремини. Међутим, механизам раздвајања у условима неравнотежног загревања још увек није довољно разјашњен. У овом истраживању испитивани су кинетички фактори који управљају микроталасно потпомогнутим фазним раздвајањем при снази микроталасног зрачења од 200 до 800 W и уделу воде од 0,12 до 0,45. Анализирани су промена температуре током времена, брзина загревања (dT/dt), запремина издвојене воде и специфична потрошња енергије. Резултати су показали изражену немонотону зависност ефикасности раздвајања од снаге микроталасног зрачења. Највећа ефикасност раздвајања постигнута је при средњим снагама од 400 до 600 W, док је даље повећање снаге довело до смањења ефикасности упркос даљем порасту температуре. Добијени резултати показују да је брзина загревања, а не крајња температура, главни параметар који управља процесом, што пружа основу за развој енергетски ефикаснијих поступака микроталасне деемулгације.

(Примљено 9. марта; ревидирано 7. маја; прихваћено 11. јуна 2026.)

REFERENCES

1. Z. Zhao, H. Li, X. Gao, *Chem. Rev.* **124** (2024) 2651–2698 (<https://doi.org/10.1021/acs.chemrev.3c00794>)
2. N. Hassanshahi, G. Hu, J. Li, *ACS Omega* **7** (2022) 33397–33407 (<https://doi.org/10.1021/acsomega.2c04022>)
3. Husain, A. A. Adewunmi, M. S. Kamal, M. Mahmoud, M. A. Al-Harhi, *Energy & Fuels* **35** (2021) 16527–16533 (<https://doi.org/10.1021/acs.energyfuels.1c02286>)
4. H. Díaz Velázquez, D. Guzmán-Lucero, R. Martínez-Palou, *J. Disp. Sci. Technol.* **44** (2023) 1884–1899 (<https://doi.org/10.1080/01932691.2022.2049293>)
5. H. Nour, M. S. Omer, S. F. Pang, *J. Appl. Sci.* **10** (2010) 2935–2939 (<https://doi.org/10.3923/jas.2010.2935.2939>)
6. L. Wei, L. Zhang, S. Guo, X. Jia, Y. Zhang, C. Sun, X. Dai, *ACS Omega* **6** (2021) 25518–25528 (<https://doi.org/10.1021/acsomega.1c03530>)
7. S. K. Nandwani, N. I. Malek, M. Chakraborty, S. Gupta, *Energy & Fuels* **34** (2020) 9411–9425 (<https://doi.org/10.1021/acs.energyfuels.0c01331>)
8. Z. Jia, Z. Niu, Z. Yang, X. Li, J. Wang, X. He, H. Sui, L. He, *Energy & Fuels* **34** (2020) 1259–1267 (<https://doi.org/10.1021/acs.energyfuels.9b02679>)

9. M. M. S. Abdullah, H. A. Al-Lohedan, *Energy & Fuels* **33** (2019) 12916–12923 (<https://doi.org/10.1021/acs.energyfuels.9b03148>)
10. O. Ezzat, A. M. Atta, H. A. Al-Lohedan, M. M. S. Abdullah, A. I. Hashem, *Energy & Fuels* **32** (2018) 214–225 (<https://doi.org/10.1021/acs.energyfuels.7b02955>)
11. D. Alves, E. Lourenço, E. Franceschi, A. F. Santos, C. C. Santana, G. Borges, C. Dariva, *Energy & Fuels* **31** (2017) 9132–9139 (<https://doi.org/10.1021/acs.energyfuels.7b01418>)
12. M. S. Bin Dahbag, M. E. Hossain, A. A. AlQuraishi, *Energy & Fuels* **30** (2016) 9260–9265 (<https://doi.org/10.1021/acs.energyfuels.6b01712>)
13. X. He, Q. Liu, Z. Xu, *Chem. Eng. Sci.* **230** (2021) 116215 (<https://doi.org/10.1016/j.ces.2020.116215>)
14. A. Adewunmi, M. S. Kamal, T. I. Solling, *J. Petrol. Sci. Eng.* **196** (2021) 107680 (<https://doi.org/10.1016/j.petrol.2020.107680>)
15. H. Bao, H. Xing, M. Liu, Q. Zhang, H. Yan, J. Liu, *J. Disp. Sci. Technol.* **41** (2020) 2116–2127 (<https://doi.org/10.1080/01932691.2019.1651204>)
16. A. Husain, M. A. Al-Harhi, *J. Petrol. Sci. Eng.* **220** (2023) 111089 (<https://doi.org/10.1016/j.petrol.2022.111089>)
17. D. S. Miller, T.-C. Kuo, D. Brennan, A. Schmitt, K. Grzesiak, R. Jenkins, H. Singh, H. Wiles, T. Martin, A. Banks, D. Hayes, R. Gupta, J. Moore, J. Mendenhall, T. Kalantar, *J. Surf. Deterg.* **28** (2025) 977–989 (<https://doi.org/10.1002/jsde.12850>)
18. Z. Song, W. Pan, S. Wang, X. Lv, X. Zhao, J. Sun, Y. Mao, X. Wang, W. Wang, *Energy Sources, Part A: Recov. Util. Environ. Eff.* **47** (2025) 9720–9739 (<https://doi.org/10.1080/15567036.2021.1956019>)
19. K. Ji, Y. Tian, J. Jiang, X. Yan, J. Tian, J. Yang, Z. He, X. Lu, *Fuel* **386** (2025) 134247 (<https://doi.org/10.1016/j.fuel.2024.134247>)
20. S. Tahami, K. Movagharnejad, *J. Mol. Liq.* **411** (2024) 125748 (<https://doi.org/10.1016/j.molliq.2024.125748>)
21. H. Sadighian, Z. Mohamadnia, E. Ahmadi, *Carbohydr. Polym.* **327** (2024) 121697 (<https://doi.org/10.1016/j.carbpol.2023.121697>)
22. F. Ye, X. Zhang, X. Jiang, H. Liu, Y. Tang, Q. Qu, L. Shen, Z. Zhang, Y. Mi, X. Yan, *Geoenergy Sci. Eng.* **230** (2023) 212265 (<https://doi.org/10.1016/j.geoen.2023.212265>)
23. P. Schacht, P. Torres-Mancera, J. Ancheyta, *Catalyst for In Situ Upgrading of Heavy Oils*. In *Catalytic In-Situ Upgrading of Heavy and Extra-Heavy Crude Oils* (Eds J. Ancheyta, M. Varfolomeev, C. Yuan) 237–262, Wiley OnLine Library (2023) (<https://doi.org/10.1002/9781119871507.ch5>)
24. M. Lei, H. Huang, J. Liu, F. Peng, *Coll. Surf. A: Physicochem. Engin. Asp.* **671** (2023) 131696 (<https://doi.org/10.1016/j.colsurfa.2023.131696>)
25. F. Song, J. Zhou, Z. Jia, L. He, H. Sui, X. Li, *J. Mol. Liq.* **382** (2023) 121864 (<https://doi.org/10.1016/j.molliq.2023.121864>)
26. K. Azizollah, *Petroleum Chemistry* **63** (2023) 338–353 (<https://doi.org/10.31857/S002824212303005X>) (in Russian)
27. T. Wei, X. Zhong, X. Chen, Z. Guo, *Langmuir* **41** (2025) 16139–16149 (<https://doi.org/10.1021/acs.langmuir.5c01225>)
28. H. Sadighian, Z. Mohamadnia, E. Ahmadi, *Langmuir* **39** (2023) 9627–9637 (<https://doi.org/10.1021/acs.langmuir.3c00564>)

29. S. Rasouli, N. Rezaei, S. Zendejboudi, X. Duan, R. L. Legge, I. Chatzis, *Langmuir* **39** (2023) 4100–4112 (<https://doi.org/10.1021/acs.langmuir.2c03480>)
30. N. Parmar, C. A. Kavale, H. Goyal, *Ind. Eng. Chem. Res.* **62** (2023) 2561–2572 (<https://doi.org/10.1021/acs.iecr.2c03877>)
31. H. Tang, L. Hao, J. Chen, F. Wang, H. Zhang, Y. Guo, *Energy & Fuels* **32** (2018) 3627–3636 (<https://doi.org/10.1021/acs.energyfuels.7b03344>)
32. T. Assenheimer, A. Barros, K. Kashefi, J. C. Pinto, F. W. Tavares, M. Nele, *Energy & Fuels* **31** (2017) 6587–6597 (<https://doi.org/10.1021/acs.energyfuels.7b00275>)
33. H. Bahmani, Y. Hojjat, A. Yazdian, M. Shirkosh, *Petrol. Sci. Technol.* **43** (2025) 1293–1309 (<https://doi.org/10.1080/10916466.2024.2326167>)
34. D. M. Hagl, D. Popovic, S. C. Hagness, J. H. Booske, M. Okoniewski, *IEEE Trans. Microw. Theory Tech.* **51** (2003) 1194–1206 (<https://doi.org/10.1109/TMTT.2003.809626>)
35. U. Kaatze, *Meas. Sci. Technol.* **18** (2007) 967–976 (<https://doi.org/10.1088/0957-0233/18/4/002>)
36. J. O. Alvarez, D. Jacobi, S. Althaus, S. Elias, *Fuel* **288** (2021) 119679 (<https://doi.org/10.1016/j.fuel.2020.119679>)
37. ASTM D7042-21a, Standard Test Method for Dynamic Viscosity and Density of Liquids by Stabinger Viscometer, ASTM International, West Conshohocken, PA, 2021 (<https://doi.org/10.1520/D7042-21A>)
38. ASTM D445-20, Standard Test Method for Kinematic Viscosity of Transparent and Opaque Liquids, ASTM International, West Conshohocken, PA, 2020 (<https://doi.org/10.1520/D0445-20>)
39. K. Paso, T. Kompalla, N. Aske, H. P. Rønningsen, J. Sjöblom, *J. Dispers. Sci. Technol.* **30** (2009) 757–781 (<https://doi.org/10.1080/01932690802643220>)
40. B. Vonnegut, *Rev. Sci. Instrum.* **13** (1942) 6–9 (<https://doi.org/10.1063/1.1769937>)
41. H. M. Princen, I. Y. Z. Zia, S. G. Mason, *J. Colloid Interface Sci.* **23** (1967) 99–107 ([https://doi.org/10.1016/0021-9797\(67\)90090-2](https://doi.org/10.1016/0021-9797(67)90090-2))
42. M. Hoorfar, A. W. Neumann, *Adv. Colloid Interface Sci.* **121** (2006) 25–49 (<https://doi.org/10.1016/j.cis.2006.06.001>)
43. S. Manholi, S. Athiyanathil, *J. Poly. Res.* **31** (2024) 1–12 (<https://doi.org/10.1007/s10965-024-04212-z>)
44. E. R. Binner, J. P. Robinson, S. A. Silvester, S. W. Kingman, E. H. Lester, *Fuel* **116** (2014) 516–521 (<https://doi.org/10.1016/j.fuel.2013.08.042>)
45. E. B. da Silva, D. Santos, M. P. de Brito, R. C. L. Guimarães, B. M. S. Ferreira, L. S. Freitas, M. C. V. de Campos, E. Franceschi, C. Dariva, A. F. Santos, M. Fortuny, *Fuel* **128** (2014) 141–147 (<https://doi.org/10.1016/j.fuel.2014.02.076>)
46. Y. Wang, C. Liu, H. Lang, Z. Hu, X. Wang, Z. Yang, Z. Wang, Z. Guo, L. Jiang, *Food Chem. X* **19** (2023) 100861 (<https://doi.org/10.1016/j.fochx.2023.100861>)
47. H. Xu, C. Hu, M. Gantumur, H. Li, N. Sukhbaatar, L. Zhang, Z. Jiang, *J. Food Eng.* **403** (2026) 112707 (<https://doi.org/10.1016/j.jfoodeng.2025.112707>)
48. Z. Li, X. Zhong, C. Luan, N. Wen, C. Shi, S. Liu, Y. Xu, Q. He, Y. Wu, J. Yang, *Food Chem. X* **21** (2024) 101149 (<https://doi.org/10.1016/j.fochx.2024.101149>)

49. L. O. Diehl, D. P. Moraes, F. G. Antes, J. S. F. Pereira, M. F. P. Santos, R. C. L. Guimarães, É. M. M. Flores, *Sep. Sci. Technol.* **46** (2011) 1358–1364 (<https://doi.org/10.1080/01496395.2011.560590>).

Accepted manuscript